Room temperature d^0 ferromagnetism in PbS films: nonuniform distribution of Pb vacancies

Journal:	*Physical Chemistry Chemical Physics*
Manuscript ID	CP-ART-07-2018-004882.R1
Article Type:	Paper
Date Submitted by the Author:	01-Nov-2018
Complete List of Authors:	Pimachev, Artem; University Of Wyoming, Physics and Astronomy Rimal, Gaurab; University of Wyoming, Physics and Astronomy Nielsen, Robert; University of Wyoming, Physics and Astronomy Tang, Jinke; University of Wyoming, Physics and Astronomy Dahnovsky, Yuri; University of Wyoming, Physics and Astronomy

Room temperature d^0 ferromagnetism in PbS films: nonuniform distribution of Pb vacancies

Artem Pimachev, Gaurab Rimal, Robert D. Nielsen, Jinke Tang, and Yuri Dahnovsky*

Department of Physics & Astronomy,/3905

1000 E. University Avenue

University of Wyoming

Laramie, WY 82071

(Dated: November 1, 2018)

Abstract

Because of the importance of ferromagnetism at room temperatures we quest for new materials that can exhibit a non-vanishing magnetic moment at room temperatures and at the same time can be used in spintronics. The experimental results indicate that d^0 ferromagnetism without any magnetic impurities takes place in PbS films made of lead sulfide 30 nm close-packed nanoparticles. To explain the existence of the d^0 ferromagnetism we propose a model where various PbS bulk and surface configurations with Pb-vacancies are analyzed. The bulk configurations have zero magnetic moments while the two surface configurations with Pb vacancies with the same non-vanishing magnetic moments and the lowest ground state energies contribute to the total magnetization. Based on the experimental value of the saturation magnetization, 0.2 emu/g, we have found that the calculated Pb vacancy concentration should be about 3.5% which is close to typical experimental values. Besides being very important for applications, there is one feature of PbS d^0 ferromagnetism that makes this material special for fundamental research; PbS ferromagnetism can exhibit topologically driven spacial magnetic moment distributions (e.g., magnetic skyrmions) due to large spin-orbit coupling.

I. INTRODUCTION

Diluted magnetic semiconductors (DMSs) have been intensively studied in the last decades to reduce or decrease the gap between spintronics and traditional electronics[1,2]. Much research has been done on II-VI and III-V DMS, especially on semiconductors doped by transition metal (TM) impurities where many unusual magnetic and optical properties have been observed in nanocrystals.[3–21]. Because of the importance of ferromagnetism at room temperature for various applications in DMSs, much research has been focused to investigate DMS materials that satisfy this criterion. Different types of dopants can substantially change the value of a magnetic moment in metal-oxide nanocrystals. For example, in In_2O_3 quantum dots (QDs) doped by Cr^{3+} impurities ferromagnetism is sensitive to QD crystal structure. Indeed, for the bcc-In_2O_3 nanocrystals the saturation magnetic moment is much greater than that of in rh-In_2O_3 quantum dots.[22] As shown in Ref.[23] different types of TM impurities can enhance or suppress the ferromagnetism in In_2O_3 or SnO_2 quantum dots. The Fe^{3+} decreases the magnetization while Mn^{2+} significantly enhances the ferromagnetism. In addition, the oxygen vacancies are able to influence the electron transport properties. In In_2O_3 nanocrystals the 2D electron mobility can be increased because of the metal-insulator transition due to the presence of O-vacancies.[24] It was theoretically predicted that room temperature ferromagnetism exists in Mn doped GaN[25] and then experimentally confirmed in Refs.[26–28]. There is another type of ferromagnetic material with T_c much above the room temperature and with no TM doping.[29–36] Such nanocrystals exhibit d^0 (d or f electrons are not involved) ferromagnetism associated with unpaired electron spins due to the intrinsic defects – vacancies. ZnO and ZnS are such nanocrystals that demonstrate d^0 ferromagnetism.[37–41]

It is known that a ZnS nanocrystal with Zn vacancies also exhibits d^0 ferromagnetism. Theoretical calculations predicted a much higher magnetization than the experimental value. .[37] Such a discrepancy was discussed in Ref.[38]. It was found that the dramatic decrease magnetization is possible due to the condensation of Zn vacancies into a droplet (or droplets). Thus, the total magnetization essentially depends on the vacancy arrangements or configurations.

There is another interesting magnetic semiconductor, zinc oxide.[30,33,42–54] ZnO nanocrystals were intensively studied, and the behavior of d^0 ferromagnetism was different. Zhi-

gang Li et al.[39] discovered the dramatic dependance of the magnetic moment on an NC size. Indeed the magnetization drops by 2-3 orders of magnitude with the nanocrystal size. Moreover, the samples become very sensitive to an oxygen rich environment that reduces the magnetization by approximately five times compared to similar experiment in vacuum. The explanation of the drop in magnetization by 2.5 orders of magnitude was provided in Ref.[40] It was found that some vacancy configurations can have large or very small (zero) magnetic moments. Thus, a vacancy distribution is extremely crucial for the creation of non-vanishing magnetization. Another important feature is where the vacancies are located, i.e., in a bulk or on the surface of a nanocrystal. It was found that the main contribution of Zn vacancies are on the surface.[40] In Ref.[41] it was shown how to identify bulk or surface vacancy locations from optical spectra.[41]

In this reseach we continue the quest for new d^0-ferromagnetic materials. The material of our study is lead sulfide. We pay much attention to lead sulfide because PbS is one of the most important narrow gap semiconductors used for infrared detectors. There is another fundamental feature of PbS – this material has large spin-orbit coupling (SOC). The large spin-orbit coupling can lead to unusual magnetic behaviors. In particular, magnetic topological structures, e.g., skyrmions, are possible in PbS crystals. As the first step of the research we experimentally observe ferromagnetism in a film made of closely packed 30 nm nanoparticles. To explain the origin of the PbS ferromagnetism we introduce a model capable of the description and understanding of the experimental data. In Ref.[21] the authors found ferromagnetism at a high transition temperature in both undoped and Mn doped PbS nanowires. Carrier-dopant exchange interaction in Mn-doped PbS quantum dots and crystals were studied by polarized light[55,56].

In this work we present the experimental proof of the existence of room temperature ferromagnetism in PbS films with Pb vacancies and provide the theoretical/computational explanation of the origin of this phenomenon. We prove that the origin of the observed ferromagnetism is the presence of Pb vacancies on a film surface. We also conclude that the Pb vacancies have to be arranged in special configurations rather than uniformly distributed over the whole PbS film.[57]

II. EXPERIMENTAL RESULTS

PbS films with thickness of about 300 nm have been deposited on Si substrates using pulsed laser deposition (PLD). The PLD target has been prepared by combining lead acetate (99.999 %, Sigma Aldrich) and sodium sulfide (99.99 %, Sigma Aldrich) in the correct proportions in aqueous solution and the precipitates have been thoroughly cleaned and dried. X-ray diffraction shows the resulting powders to be in PbS rock-salt phase. The powders have been ground and cold pressed to make a target for the PLD. The details on the film preparation can be found in the references[58,59]. We have done the extensive XRD analyses of the samples. The standard PbS peaks, along with extra peak from Pb (the peaks at 31.5° and 36° (marked with an asterisk), are shown in Fig. 1. After annealing, the lattice constant decreases from 5.92 Å to 5.89 Å as shown in Fig. 1 by the peak shift to higher 2-θ angle. This shift is likely due to the creation of the vacancies during annealing. Note that the sample has been cut after the preparation and the latter piece has been used for annealing. The decrease of the intensity in the XRD data is due to the use of a smaller slit during measurements. The overall grain size remains approximately similar after annealing as shown in Fig. 1 from the similar peak width.

The films have been also characterized using scanning electron microscopy (SEM) and atomic force microscopy (AFM). The average particle size of PbS was found to be about 30 nm as determined from AFM measurements. XRD confirms the rock-salt phase of the films, although there is an impurity phase of Pb metal present in the samples, which is inherent to the preparation method. The presence of these Pb clusters have an important consequence in Pb vacancy formation and therefore, in the magnetic properties of the films of 30 nm close-packed nanoparticle.Heating in a high vacuum environment helps to create vacancies, therefore we have done the annealing experiments to test the effects of vacancies. Annealing has been done in the same vacuum chamber after the initial deposition. The sample has been cut and then mounted into the chamber where it has been heated to 400° C and annealed at pressure of $\sim$ 10 μTorr for 12 hrs. The magnetic measurements have been done with a Quantum Design's PPMS system.

Figs. 2 (a) and (b) demonstrate the magnetic hysteresis loop of the as deposited film and annealed film measured at room temperature. As seen, from Fig. 2, the annealed samples are ferromagnetic at room temperature with the coercivity $H_c \sim 35$ Öe. The saturation

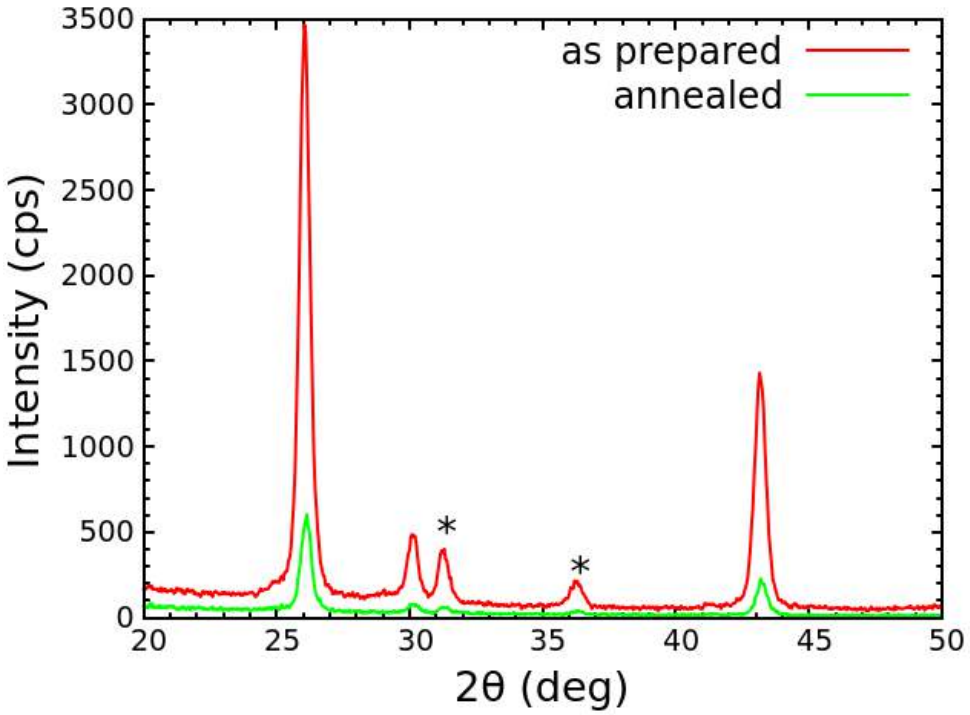

FIG. 1: X-ray diffraction pattern of as prepared and annealed samples.

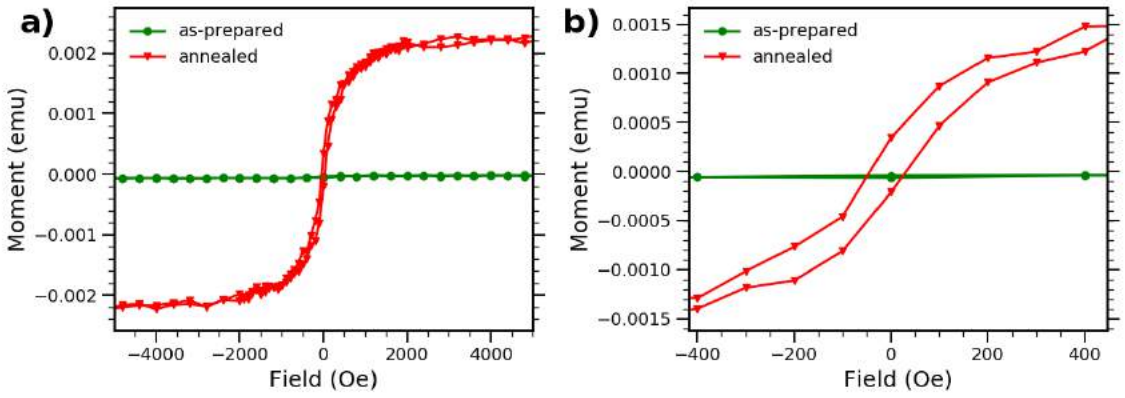

FIG. 2: (a) Magnetic hysteresis for as-prepared and annealed PbS at room temperature. (b) Magnified view of the hysteresis shown in (a).

magnetization of the as prepared sample is about $2 \cdot 10^{-2}\ emu/g$, and that of the annealed sample is $2 \cdot 10^{-1}\ emu/g$. When the as prepared film is annealed in vacuum, the saturation magnetization increases.

It is anticipated that during the annealing, the high vapor pressure of sulfur leads to its removal and thus, creates sulfur vacancies. This seems to contradict our understanding of Pb vacancy-induced ferromagnetism. To address this issue, we performed energy calculations on the migration of Pb atoms as a result of the presence of S vacancies as demonstrated in Fig. 3.

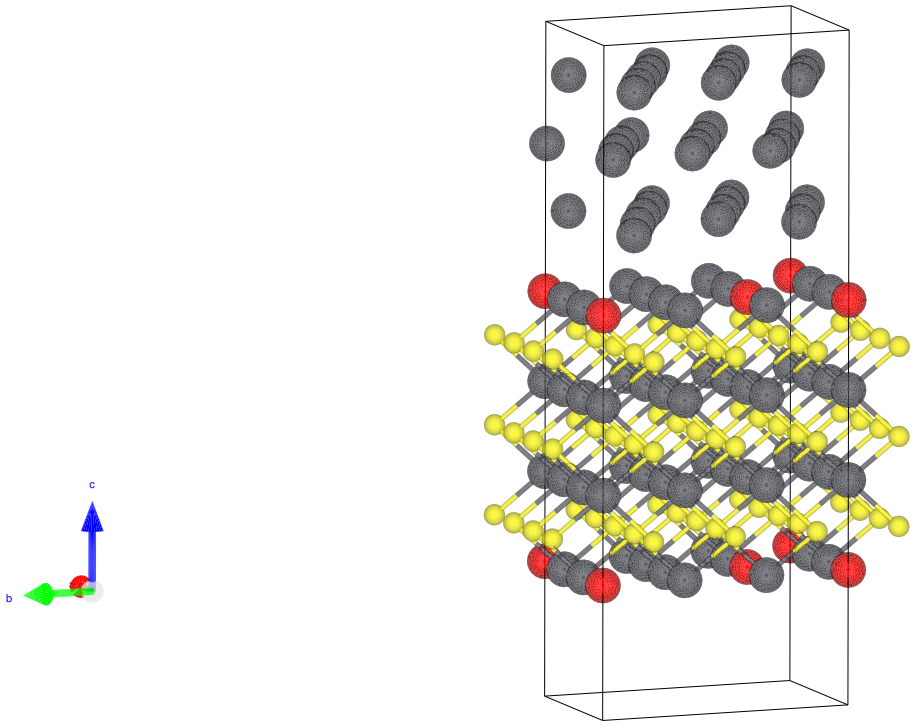

FIG. 3: Pb metal layers are on the surface with PbS crystal with vacancies underneath. Pb atoms are in gray, sulfur are in yellow, and lead vacancies are in red colors.

The calculations have found that Pb atoms located in the vicinity of a Pb metal cluster have the tendency to migrate to the Pb-layer creating the Pb vacancies in the PbS crystal.. We have computationally found that this physical picture is energetically favorable. Indeed, the energy for the state where Pb atoms from the PbS crystal migrate to the Pb cluster surface (see Fig. 3) is lower by 1.85 eV per Pb-atom compared to when the Pb atoms stay in the PbS crystal. With the annealing this creates an additional local magnetic moment leading to the enhancement of the saturation magnetization.

III. COMPUTATIONAL DETAILS

To explain the experimental data we propose a model that consists of the both bulk and surface Pb vacancy configurations, each with the unique Pb vacancy groups. The first principle calculations have been performed using the Vienna Ab Initio Simulation Package (VASP)[60–64] and ELK FP-LAPW codes[62,64–67]. For the VASP calculations we employ the General Gradient Algorithm (GGA) with the PBE exchange-correlation functional[68–72] that includes the spin polarization and tetrahedron smearing[73]. For the PAW pseudopotentials[60,61,74] an energy cutoff of 400 eV is employed. The geometries of all vacancy configurations have been optimized within VASP to the accuracy of 0.1 meV. To find a spatial magnetization density distribution we have used the ELK FP-LAPW codes[65]. The magnetization vector field over a supercell for a bulk PbS crystal, in which the Pb vacancies induce a high magnetic moment, has been investigated within the latter code. For these calculations, the muffin-tin radii of Pb and S have been chosen as 1.42 Å and 1.12 Å respectively. We have also included spin-orbit coupling (SOC) in the second-variational procedure[75,76] to an accuracy of 10 meV. Muffin-tin wavefunctions with the angular momentum up to $L = 14\ \hbar$ are included. For a higher accuracy in the magnetization calculations we have included ten additional unoccupied states as recommended in Ref.[65].

IV. RESULTS AND DISCUSSIONS

The main goal of the theoretical investigation is to explain the experimentally observed room temperature d^0 ferromagnetism in PbS films. We have checked many Pb-vacancy configurations with one, two, three, four, and five Pb vacancies in the extended unit cell $(3 \times 3 \times 3)$ in the bulk and on the surface of the film and found that the one, two, three, and four Pb-vacancy configurations provide antiferromagnetism with a zero magnetic moment. Therefore, they should be disregarded as contradictive to the experimental data. Only five Pb-vacancy configurations provide ferromagnetism explaining the experimental data. We have then found their ground state energies and compared them with each other. The configuration with the lowest ground state energy has to be selected as the proper configuration to explain the experimental data. If it happens that a configuration with the lowest ground state energy has a zero magnetic moment, this configuration has to be disregarded because

	Bulk A	Bulk B	Bulk C	Bulk D	Bulk E	Bulk F
Energy, eV	-206.37	-206.60	-206.33	-206.87	-206.34	-205.88
Moment, μ_B	0.00	0.00	0.00	0.00	0.00	0.83
ΔE, eV	0.50	0.27	0.54	0.00	0.53	0.99
$\Delta E_{Full}/Vac$, eV	6.08	6.03	6.09	5.98	6.08	6.18

TABLE I: Energy and magnetic moment results of the DFT calculations for the bulk configurations shown in Fig. 4.

it cannot explain the experimental non-zero value of the magnetization.

First, we study the bulk configurations. The schematic pictures of these configurations are presented in Fig. 4.

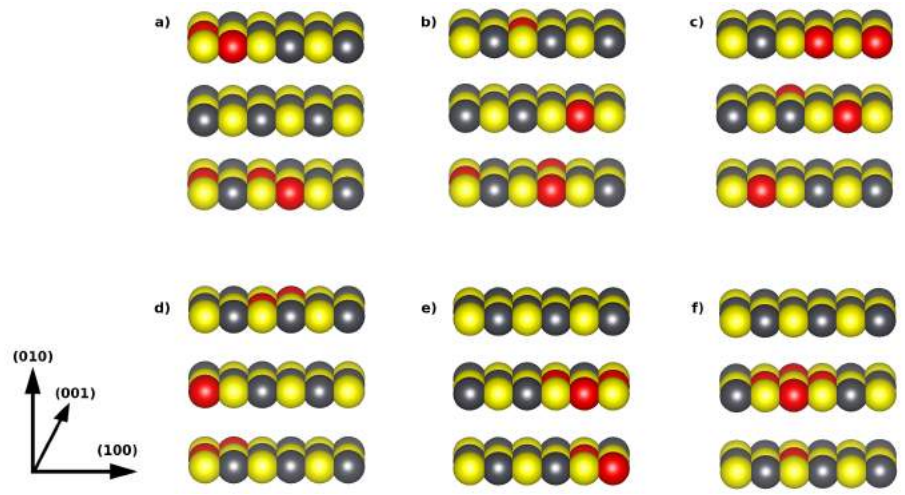

FIG. 4: Bulk Pb-vacancy configurations in a PbS crystal. Pb atoms shown are shown in gray with sulfur atoms shown in yellow and Pb-vaccacy locations for each configuration shown in red.

The ground-state energies and magnetic moments calculated in VASP are presented in Table I for selected five Pb-vacancy bulk configurations.

In Table I the only configuration with a non-vanishing magnetic moment is configuration Bulk F. This configuration is shown in Fig. 5 in more detail matching a similar picture presented in Fig. 4 F. However, the configuration with the lowest ground state energy is different. It is configuration Bulk D. The energy difference between configurations Bulk D and F is 1 eV. Taking into account that the bulk vacancy configurations contain five vacancies we have found the energy per vacancy, ΔE. The energy per vacancy difference between

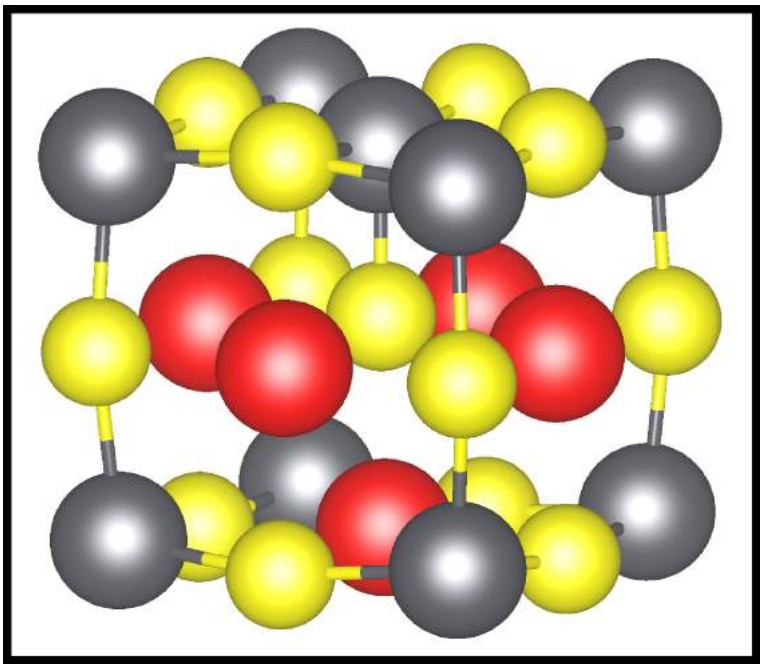

FIG. 5: Bulk vacancy configuration Bulk F that provides a non-vanishing magnetic moment.

the above mentioned Pb-vacancy configurations is 0.2 eV. Such a difference is greater than k_BT and therefore, the Bulk D configuration with the zero magnetization is more favorable. Thus, the bulk vacancy configurations are not able to explain the experiment.

The energy, ΔE, and the relative energy differences per vacancy are defined as a difference between the total energy of a supercell with vacancies and the total energy of supercell without vacancies. For the relative energy difference per vacancy we divide the energy differences by the number of vacancies, N_{vac} in a supercell. As mentioned above, there are five vacancies in the bulk and four vacancies in the surface configurations. The relative energy difference $\Delta E_{full}/N_{vac}$ is defined by the following equation:

$$\frac{\Delta E_{full}}{N_{vac}} = \frac{E_{full} - E_{config}}{N_{vac}}. \quad (1)$$

Since the bulk configuration with the lowest energy has been antiferromagnetic, the next step is to study the surface Pb-vacancy configurations shown in Fig. 6.

We calculate four different surface configurations with Pb and S surface terminations presented in Figs. 6 and 7. For all vacancy configurations we have calculated magnetic moments and ground state energies . The results are given by Table II. Both configurations

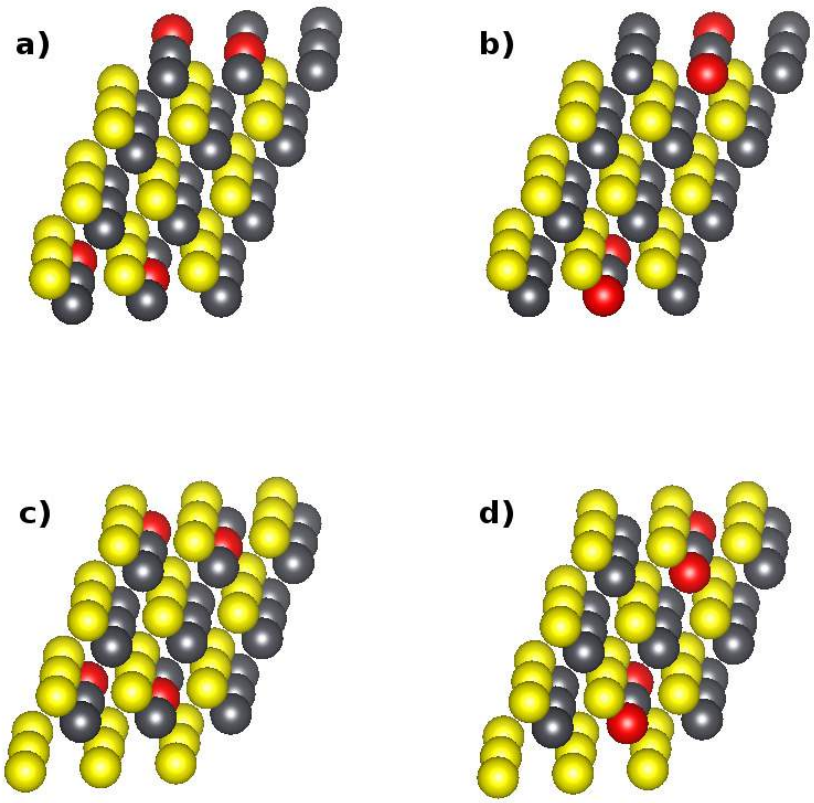

FIG. 6: Surface Pb-vacancy configurations. Pb atoms shown are shown in gray with sulfur atoms shown in yellow and Pb-vaccacy locations for each configuration shown in red. (a) and (b) are Pb terminated and (c) and (d) are S terminated.

Surface A and Surface B, shown in Fig. 8, provide a non-vanishing magnetization with the lowest ground state energy.

In this table Surface A and B vacancy configurations represent the Pb-surface terminations while Surface C and D vacancy configurations denote the S-surface terminations as shown in Fig. 6. From Table II we see now that there are several vacancy configurations that have non-vanishing magnetizations. They are configurations Surface A, B, and C. Then we verify their ground state energies. We find that configurations Surface A and B have the lowest ground state energies. These configurations have almost the same magnetic moment per vacancy and both contribute to the total film magnetization.

Having identified the most probable surface vacancy configurations, we compare their ground state energies with the bulk configuration energies. Because the bulk and surface

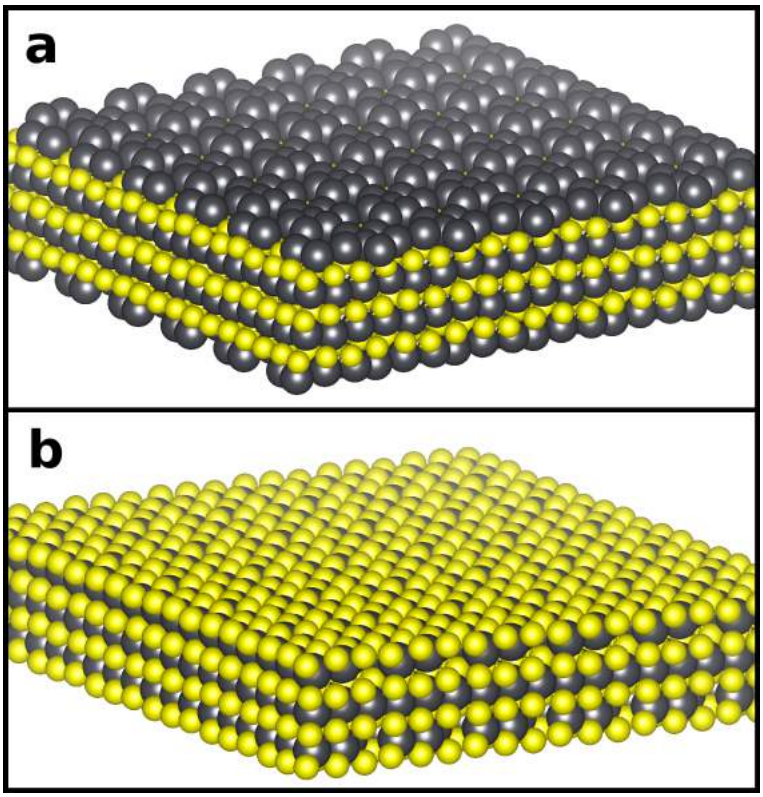

FIG. 7: Surface layer with (a) Pb and (b) S surface terminations, respectively.

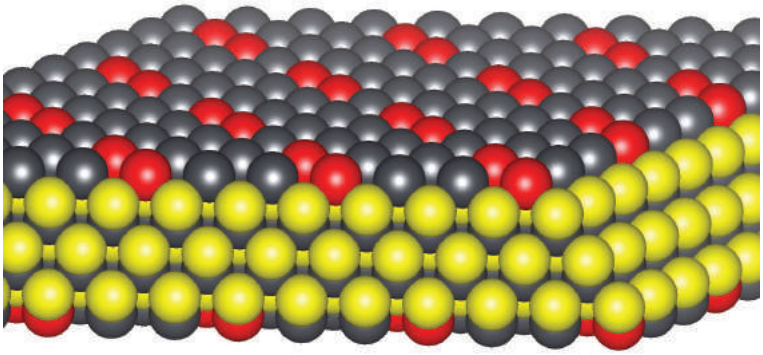

FIG. 8: Surface Pb vacancy configuration Surface A with the vacancies shown in red color.

unit cells contain different numbers of vacancies: five for the bulk and four for the surface, we calculate the energy per vacancy as described by Eq. 1. From the comparison of ground state energies for configurations Bulk D and Surface A and B we conclude that the surface configurations are much more favorable with the ground state energy difference about 3.3 eV.

In the experiments the film is made of close-packed nanoparticles of about 30 nm in size.

	Surface A	Surface B	Surface C	Surface D
Energy, eV	-246.49	-246.49	-235.11	-236.19
Moment, μ_B	1.40	1.40	0.92	0.00
ΔE, eV	0.00	0.00	11.38	10.30
$\Delta E_{Full}/Vac$, eV	2.87	2.87	6.74	6.47

TABLE II: Energy and magnetic moment results of DFT calculations for surface configurations shown in Fig. 6.

Considering a spherical nanoparticle we have estimated the concentration of vacancies to fit the experimental value of the magnetization per volume. Based on the experimentally measured saturation magnetization, the PbS slab size, and magnetic moment per surface vacancy (seeTable II), we have found that the estimated concentration of Pb vacancies is about 3.5% which is close to a typical experimental value.[77]

In the experiment there has been the observation of Pb-metal islands. This picture is confirmed by the calculations that are in favor of a Pb rather than S surface terminations.

We have also verified the magnetization value in the presence of S-vacancies. We have found that the magnetic moment vanishes in this case .

V. CONCLUSIONS

As it was believed before[57] the magnetic moment in a PbS nanocrystal is zero indicating the antiferromagnetic arrangement. However, non-zero value of the magnetization has been observed in the experiments where the magnetization dependence on an applied magnetic field is shown in Figs. 2 (a) and (b). To explain the experimental data we have proposed a model where some special configurations of Pb-vacancies can exhibit non-vanishing magnetic moments. In this model we have considered six bulk Pb vacancy configurations (see Fig. 4 and also Table I) and found that the configuration with the lowest ground state energy is configuration Bulk D. However, this configuration has a zero magnetic moment and cannot explain the experimental non-zero magnetization value. We then studied surface configurations (see Fig. 6) in two different cases with Pb and S terminations (see Fig. 7). We have found that two configurations Surface A and B shown in Fig. 6 have the lowest ground state energies with non-zero magnetic moments (see Table II). It is interesting to

note that the contribution of these configurations are equal however, they are two very different configurations. Based on the experimental value of the magnetization, 0.2 emu/g, we have estimated the concentration of vacancies in the experiments described in the experimental section. We have found that the calculated Pb vacancy concentration should be about 3.5% which is within the typical experimental value range (2% - 8%). Room temperature d^0 ferromagnetism in PbS films can be used in different practical areas such as spintronic based devices, magnetic recording of information in computers, etc. There is one feature of PbS d^0 ferromagnetism that makes this material special for fundamental research. PbS ferromagnetism can exhibit topologically driven spacial magnetic moment distributions (e.g., magnetic skyrmions) because of large spin-orbit coupling.

Acknowledgments

This work has been supported by a grant (No. DMR-1710512.) from the U.S. National Science Foundation to the University of Wyoming.

---

* Electronic address: yurid@uwyo.edu

[1] A. H. MacDonald, P. Schiffer, and N. Samarth, *Nature Materials*, 2005, **4**(3), 1325.

[2] T. Dietl and H. Ohno, *Reviews of Modern Physics*, 2014, **86**(1), 187–251.

[3] D. Hoffman, B. Meyer, A. Ekimov, I. Merkulov, A. L. Efros, M. Rosen, G. Couino, T. Gacoin, and J. Boilot, *Solid State Communications*, 2000, **114**(10), 547–550.

[4] B. B. Srivastava, S. Jana, N. S. Karan, S. Paria, N. R. Jana, D. Sarma, and N. Pradhan, *The Journal of Physical Chemistry Letters*, 2010, **1**(9), 1454–1458.

[5] R. Bhargava, D. Gallagher, X. Hong, and A. Nurmikko, *Physical Review Letters*, 1994, **72**(3), 416.

[6] A. Bol and A. Meijerink, *Physical Review B*, 1998, **58**(24), R15997.

[7] J. Suyver, S. Wuister, J. Kelly, and A. Meijerink, *Physical Chemistry Chemical Physics*, 2000, **2**(23), 5445–5448.

[8] D. J. Norris, N. Yao, F. T. Charnock, and T. A. Kennedy, *Nano Letters*, 2001, **1**(1), 3–7.

[9] D. W. Langer and H. J. Richter, *Physical Review*, 1966, **146**(2), 554.

[10] N. Pradhan and X. Peng, *Journal of the American Chemical Society*, 2007, **129**(11), 3339–3347.

[11] M. A. Malik, P. O'Brien, and N. Revaprasadu, *Journal of Materials Chemistry*, 2001, **11**(9), 2382–2386.

[12] S. Salimian and S. F. Shayesteh, *Journal of Superconductivity and Novel Magnetism*, 2012, **25**(6), 2009–2014.

[13] V. Proshchenko and Y. Dahnovsky, *The Journal of Physical Chemistry C*, 2014, **118**(48), 28314–28321.

[14] V. Proshchenko and Y. Dahnovsky, *Physica Status Solidi (b)*, 2015, **252**(10), 2275–2279.

[15] A. Pimachev and Y. Dahnovsky, *The Journal of Physical Chemistry C*, 2015, **119**(29), 16941–16946.

[16] V. Proshchenko and Y. Dahnovsky in *Photoinduced Processes at Surfaces and in Nanomaterials;* ACS Publications, 2015; pp. 117–135.

[17] V. Proshchenko and Y. Dahnovsky, *Physical Chemistry Chemical Physics*, 2015, **17**(40), 26828–26832.

[18] M. Kan, J. Zhou, Q. Sun, Y. Kawazoe, and P. Jena, *The Journal of Physical Chemistry Letters*, 2013, **4**(20), 3382–3386.

[19] K. Schouteden, T. Ivanova, Z. Li, V. Iancu, E. Janssens, and C. Van Haesendonck, *The Journal of Physical Chemistry Letters*, 2015, **6**(6), 1048–1052.

[20] A. Saha, A. Shetty, A. Pavan, S. Chattopadhyay, T. Shibata, and R. Viswanatha, *The Journal of Physical Chemistry Letters*, 2016, **7**(13), 2420–2428.

[21] S. K. Mandal, A. R. Mandal, and S. Banerjeet, *ACS Appl. Mater. Interfaces*, 2012, **4**, 205–209.

[22] S. S. Farvid, M. Hegde, and P. V. Radovanovic, *Chemistry of Materials*, 2013, **25**(2), 233–244.

[23] N. S. Garnet, V. Ghodsi, L. N. Hutfluss, P. Yin, M. Hegde, and P. V. Radovanovic, *The Journal of Physical Chemistry C*, 2017, **121**(3), 1918–1927.

[24] A. Walsh, *Applied Physics Letters*, 2011, **98**(26), 261910.

[25] T. Dietl, H. Ohno, F. Matsukura, J. Cibert, and D. Ferrand, *Science*, 2000, **287**(5455), 1019–1022.

[26] M. L. Reed, N. A. El-Masry, H. H. Stadelmaier, M. K. Ritums, M. J. Reed, C. A. Parker, J. C. Roberts, and S. M. Bedair, *Applied Physics Letters*, 2001, **79**(21), 3473–3475.

[27] P. Sharma, A. Gupta, K. V. Rao, F. J. Owens, R. Sharma, R. Ahuja, J. M. O. Guillen, B. Johansson, and G. A. Gehring, *Nature Materials*, 2003, **2**(10), 984.

[28] P. Dev, Y. Xue, and P. Zhang, *Physical review letters*, 2008, **100**(11), 117204.

[29] M. Venkatesan, C. Fitzgerald, and J. Coey, *Nature*, 2004, **430**(7000), 630.

[30] A. Sundaresan, R. Bhargavi, N. Rangarajan, U. Siddesh, and C. Rao, *Physical Review B*, 2006, **74**(16), 161306.

[31] N. H. Hong, J. Sakai, N. Poirot, and V. Brizé, *Physical Review B*, 2006, **73**(13), 132404.

[32] H. Pan, J. Yi, L. Shen, R. Wu, J. Yang, J. Lin, Y. Feng, J. Ding, L. Van, and J. Yin, *Physical Review Letters*, 2007, **99**(12), 127201.

[33] D. Gao, G. Yang, J. Zhang, Z. Zhu, M. Si, and D. Xue, *Applied Physics Letters*, 2011, **99**(5), 052502.

[34] Z. Zhang, U. Schwingenschlögl, and I. S. Roqan, *RSC Advances*, 2014, **4**(92), 50759–50764.

[35] G. Zhu, S. Zhang, Z. Xu, J. Ma, and X. Shen, *Journal of the American Chemical Society*, 2011, **133**(39), 15605–15612.

[36] W.-Z. Xiao, L.-l. Wang, Q.-Y. Rong, G. Xiao, and B. Meng, *Journal of Applied Physics*, 2014, **115**(21), 213905.

[37] V. Proshchenko, A. Karanovich, and Y. Dahnovsky, *The Journal of Physical Chemistry C*, 2016, **120**(20), 11253–11261.

[38] V. Proshchenko and Y. Dahnovsky, *Journal of Physics: Condensed Matter*, 2016, **29**(2), 025803.

[39] Z. Li, W. Zhong, X. Li, H. Zeng, G. Wang, W. Wang, Z. Yang, and Y. Zhang, *Journal of Materials Chemistry C*, 2013, **1**(41), 6807–6812.

[40] A. Pimachev, V. Proshchenko, and Y. Dahnovsky, *The Journal of Physical Chemistry C*, 2017, **121**(35), 19401–19406.

[41] A. Pimachev, V. Proshchenko, S. Horoz, O. Sahin, and Y. Dahnovsky, *Solid State Communications*, 2017, **257**, 47–49.

[42] M. Khalid, M. Ziese, A. Setzer, P. Esquinazi, M. Lorenz, H. Hochmuth, M. Grundmann, D. Spemann, T. Butz, and G. Brauer, *Physical Review B*, 2009, **80**(3), 035331.

[43] B. B. Straumal, A. A. Mazilkin, S. G. Protasova, A. A. Myatiev, P. B. Straumal, G. Schütz, P. A. Van Aken, E. Goering, and B. Baretzky, *Physical Review B*, 2009, **79**(20), 205206.

[44] C. Peng, Y. Liang, K. Wang, Y. Zhang, G. Zhao, and Y. Wang, *The Journal of Physical Chemistry C*, 2012, **116**(17), 9709–9715.

[45] H. Zeng, C. Zhi, Z. Zhang, X. Wei, X. Wang, W. Guo, Y. Bando, and D. Golberg, *Nano letters*, 2010, **10**(12), 5049–5055.

[46] Q. Wang, Q. Sun, G. Chen, Y. Kawazoe, and P. Jena, *Physical Review B*, 2008, **77**(20), 205411.

[47] K. E. Knutsen, A. Galeckas, A. Zubiaga, F. Tuomisto, G. C. Farlow, B. G. Svensson, and A. Y. Kuznetsov, *Physical Review B*, 2012, **86**(12), 121203.

[48] H. Kaftelen, K. Ocakoglu, R. Thomann, S. Tu, S. Weber, and E. Erdem, *Physical Review B*, 2012, **86**(1), 014113.

[49] H. Zeng, X. Xu, Y. Bando, U. K. Gautam, T. Zhai, X. Fang, B. Liu, and D. Golberg, *Advanced Functional Materials*, 2009, **19**(19), 3165–3172.

[50] G. Xing, D. Wang, J. Yi, L. Yang, M. Gao, M. He, J. Yang, J. Ding, T. C. Sum, and T. Wu, *Applied Physics Letters*, 2010, **96**(11), 112511.

[51] I. Lorite, B. Straube, H. Ohldag, P. Kumar, M. Villafuerte, P. Esquinazi, C. E. Rodriguez Torres, S. Perez de Heluani, V. Antonov, and L. Bekenov, *Applied Physics Letters*, 2015, **106**(8), 082406.

[52] M. Khalid and P. Esquinazi, *Physical Review B*, 2012, **85**(13), 134424.

[53] P. Esquinazi, W. Hergert, D. Spemann, A. Setzer, and A. Ernst, *IEEE Transactions on Magnetics*, 2013, **49**(8), 4668–4674.

[54] R. Viswanatha, D. Naveh, J. R. Chelikowsky, L. Kronik, and D. D. Sarma, *The Journal of Physical Chemistry Letters*, 2012, **3**(15), 2009–2014.

[55] G. Long, B. Barman, S. Delikanli, Y. Tsung Tsai, P. Zhang, A. Petrou, and H. Zeng, *Applied physics letters*, 2012, **101**(6), 062410.

[56] L. Turyanska, J. Blokland, U. Elfurawi, O. Makarovsky, P. Christianen, and A. Patanè, *Physical Review B*, 2010, **82**(19), 193302.

[57] A. Pimachev and Y. Dahnovsky, *The Journal of Physical Chemistry C*, 2015, **119**(29), 16941–16946.

[58] G. Rimal, A. K. Pimachev, A. J. Yost, U. Poudyal, S. Maloney, W. Wang, T. Chien, Y. Dahnovsky, and J. Tang, *Applied Physics Letters*, 2016, **109**(10), 103901.

[59] G. Rimal and J. Tang, *Scientific Reports*, 2017, **7**, 42224.

[60] G. Kresse and J. Furthmüller, *Computational Materials Science*, 1996, **6**(1), 15–50.

[61] G. Kresse and J. Furthmüller, *Physical Review B*, 1996, **54**(16), 11169–11186.

[62] W. Kohn and L. J. Sham, *Physical Review*, 1965, **140**(4A).

[63] J. Hafner, *Journal of Computational Chemistry*, 2008, **29**(13), 2044–2078.

[64] J. C. Slater, *Physical Review*, 1937, **51**(10), 846–851.

[65] D. J. Singh and L. Nordstrom, *Planewaves, Pseudopotentials, and the LAPW Method*, Springer,

2006.

[66] M. Weinert, G. Schneider, R. Podloucky, and J. Redinger, *Journal of Physics: Condensed Matter*, 2009, **21**(8), 084201.

[67] P. M. Marcus, *International Journal of Quantum Chemistry*, 2009, **1**(S1), 567–588.

[68] J. P. Perdew, K. Burke, and M. Ernzerhof, *Physical Review Letters*, 1996, **77**(18), 3865–3868.

[69] P. E. Blochl, *Physical Review B*, 1994, **50**(24), 17953–17979.

[70] J. P. Perdew, *Physical Review B*, 1986, **33**(12), 8822–8824.

[71] J. P. Perdew, *AIP Conference Proceedings*, 2001.

[72] J. P. Perdew, J. A. Chevary, S. H. Vosko, K. A. Jackson, M. R. Pederson, D. J. Singh, and C. Fiolhais, *Physical Review B*, 1993, **48**(7), 4978–4978.

[73] P. E. Blöchl, O. Jepsen, and O. K. Andersen, *Physical Review B*, 1994, **49**(23), 16223–16233.

[74] G. Kresse and D. Joubert, *Physical Review B*, 1999, **59**(3), 1758–1775.

[75] C. Li, A. J. Freeman, H. J. F. Jansen, and C. L. Fu, *Physical Review B*, 1990, **42**(9), 5433–5442.

[76] D. D. Koelling and B. N. Harmon, *Journal of Physics C: Solid State Physics*, 1977, **10**(16), 3107.

[77] S. Christensen, N. Bindzus, M. Sist, M. Takata, and B. B. Iversen, *Physical Chemistry Chemical Physics*, 2016, **18**(23), 15874–15883.

We experimentally find room temperature ferromagnetism in PbS nanoparticle and theoretically attribute this due to Pb-vacanices located on the surface.